

# Equilibrated Diffusion: Frequency-aware Textual Embedding for Equilibrated Image Customization

Liyuan Ma  
Westlake University  
Hangzhou, China  
maliyuan@westlake.edu.cn

Xueji Fang  
Zhejiang University  
Westlake University  
Hangzhou, China  
fangxueji@zju.edu.cn

Guo-Jun Qi\*  
Westlake University  
Hangzhou, China  
guojunq@gmail.com



**Figure 1: Image customization results of our method, which enables the recreation of a specified conceptual subject under unstylized text guidance, while also providing the flexibility to dynamically edit the subject with challenging stylized prompt.**

## ABSTRACT

Image customization involves learning the subject from provided concept images and generating it within textual contexts, typically yielding alterations of attributes such as style or background. Prevaling methods primarily rely on fine-tuning technique, wherein a unified latent embedding is employed to characterize various concept attributes. However, the attribute entanglement renders customized result challenging to mitigate the influence of subject-irrelevant attributes (e.g., style and background). To overcome these issues, we propose Equilibrated Diffusion, an innovative method that achieves equilibrated image customization by decoupling entangled concept attributes from a frequency-aware perspective, thus harmonizing textual and visual consistency. Unlike conventional approaches that employ a shared latent embedding and tuning process to learn concept, our Equilibrated Diffusion draws inspiration

from the correlation between high- and low-frequency components with image style and content, decomposing concept accordingly in the frequency domain. Through independently optimizing concept embeddings in the frequency domain, the denoising model not only enriches its comprehension of style attribute irrelevant to subject identity but also inherently augments its aptitude for accommodating novel stylized descriptions. Furthermore, by combining different frequency embeddings, our model retains the spatially original customization capability. We further design a diffusion process guided by subject masks to alleviate the influence of background attribute, thereby strengthening text alignment. To ensure subject-related information consistency, Residual Reference Attention (RRA) is incorporated into the denoising model of spatial attention computation, effectively preserving structural details. Experimental results demonstrate that Equilibrated Diffusion surpasses other competitors with better subject consistency while closely adhering to text descriptions, thus validating the superiority of our approach. The code is available at <https://github.com/MAPLE-AIGC/EqDiff>.

\*Guo-Jun Qi is the corresponding author.

Permission to make digital or hard copies of all or part of this work for personal or classroom use is granted without fee provided that copies are not made or distributed for profit or commercial advantage and that copies bear this notice and the full citation on the first page. Copyrights for components of this work owned by others than the author(s) must be honored. Abstracting with credit is permitted. To copy otherwise, or republish, to post on servers or to redistribute to lists, requires prior specific permission and/or a fee. Request permissions from [permissions@acm.org](mailto:permissions@acm.org).  
MM '24, October 28–November 1, 2024, Melbourne, VIC, Australia

© 2024 Copyright held by the owner/author(s). Publication rights licensed to ACM.  
ACM ISBN 979-8-4007-0686-8/24/10  
<https://doi.org/10.1145/3664647.3680729>

## CCS CONCEPTS

• Computing methodologies → Computer vision.

## KEYWORDS

Image Customization, Diffusion Model, Fourier Transformation

**ACM Reference Format:**

Liyuan Ma, Xueji Fang, and Guo-Jun Qi. 2024. Equilibrated Diffusion: Frequency-aware Textual Embedding for Equilibrated Image Customization. In *Proceedings of the 32nd ACM International Conference on Multimedia (MM '24)*, October 28–November 1, 2024, Melbourne, VIC, Australia. ACM, New York, NY, USA, 9 pages. <https://doi.org/10.1145/3664647.3680729>

**1 INTRODUCTION**

Text-to-Image (T2I) customization aims to customize a Text-to-Image diffusion model using a handful of provided concept images to generate diverse images aligned with the target prompts. This technology can support a variety of downstream applications, spanning from virtual photography to personalized e-commerce product design. It is noteworthy that the primary challenge in this task lies in striking a balance between maintaining consistency in the subject identity and coherence with the target prompts.

Current T2I customization paradigm mainly encompasses two main approaches: model finetuning and encoder-based pretraining. Encoder-based approaches [12, 43, 47] usually leveraged large-scale datasets tailored to specific domains to learn concepts. However, these methods face challenges in generalization across diverse domains and necessitate substantial image datasets, thereby compromising their adaptability. In contrast, finetuning-based methods [1, 11, 20, 24, 32, 42] established associations between concept and latent textual embedding through denoising optimization. However, textual representations are constrained to overfit given concept and lead to entanglement with identity-unrelated style and background attributes, which undermines its capacity to accommodate new textual descriptions during customization. Although some works [3, 6] aim to mitigate the interference of identity-related information by leveraging distinct embeddings. They primarily focus on spatial attributes such as pose and are unable to address the influence of style attribute. Furthermore, textual representations lack spatial expressiveness, resulting in poor image alignment. We attribute the challenge of achieving the trade-off between image and stylized prompt-alignment in customization to the interplay between content and style during the optimization. This interplay necessitates the fitting of model parameters representing specific concepts to both content and style, making it difficult to prevent identity-related attribute from being influenced by the style attribute of original concept image.

In this paper, we propose Equilibrated Diffusion to address aforementioned issues, which succeed in image- and text-aligned customization as shown in fig. 1. It incorporates a comprehensive training strategy comprising Frequency-aware Decoupled Textual Embedding (FDTE) and a Mask Guided Diffusion Process (MGDP) to enhance text-alignment by disentanglement between identity-irrelevant attributes (e.g., style and background) with identity-relevant one, along with the Residual Reference Attention (RRA) to enhance image alignment. Motivated by the fact that image style and content can be represented by high- and low-frequency components [15], FDTE decouples the concept into different textual embeddings, each bound to the denoising process of different frequency bands of the input image. Through the independent optimization of content and style embeddings and denoising learning applied to image inputs across various frequency bands, the denoising model not only enhances its understanding of style attributes

unrelated to subject identity but also intrinsically augments its ability to accommodate novel stylized descriptions as evidenced by results presented in fig. 8. Furthermore, MGDP utilizes the mask of subject to restrict concept denoising learning in the subject region, allowing the model to focus on learning the subject's concept and eliminate background interference. Finally, to improve the spatial details preservation of subject concept, our proposed RRA employs a spatial attention mechanism to explicitly inject spatial structural details from encoded reference into denoising features.

In summary, our approach aims to achieve subject consistency and alignment with textual descriptions in the customization of image concepts, offering the following contributions. Firstly, we propose FDTE and MGDP in our training strategy to mitigate interference from irrelevant attributes such as style and background on concepts. These techniques aid the model in learning identity-related concepts while excluding interference from style and background attributes irrelevant to identity. Secondly, we design RRA to preserve texture details of the subject concept in generated images with spatial attention mechanisms. Finally, we demonstrate that Equilibrated Diffusion outperforms prior methods in achieving consistency between identity and prompt, showing qualitative and quantitative advantages.

**2 RELATED WORK****2.1 Diffusion-based Text-to-Image Generation**

Diffusion models [16, 31, 36, 38] constitute a category of generative models that learn to simulate the generation process through sequential denoising process, which restores the noisy data disturbed by forward diffusion. Significant advancements have been achieved in image generation based on diffusion models. Subsequent endeavors have focused on enhancing the controllability of generated outputs by incorporating additional conditional information [41, 44] (such as semantic map, sketch, and text, etc.) to govern the generation process. Among these, text conditioning inherently offers superior editability and flexibility. Concurrently, with advancements in large language models, the understanding of text has also improved, thereby fostering the development of text-to-image generation models [25, 29, 33]. Nevertheless, despite the potential for diverse image generation guided by text, text-conditioned image generation models encounter difficulties in tailored image synthesis related to specific concepts. Customizing images entails preserving the identity information correlated with the provided textual descriptions, posing a significant challenge for text-to-image generation models.

**2.2 Image Customization**

Leveraging the power of text-to-image diffusion model, image customization [1–3, 6, 10–13, 20, 24, 32, 42] has witnessed rapid development in controllability and faithfulness. Given a set of concept images, image customization is designed to produce new images of a given subject that adhere to textual descriptions. The core of image customization largely revolves around the adjustment of parameters within the foundational text-to-image generation model or incorporating additional parameters. Such modifications involves fine-tuning text embedding [1, 11, 42], adjusting parameters within the full or partial U-Net network [8, 23, 32, 39], as well

as integrating extra encoder components [7, 9, 14, 18, 34, 43, 45, 47]. Early methods [1, 10, 11, 13, 42] capture the concept of the subject through text embeddings represented by specific token. Typically, Textual Inversion [11] encapsulates the concept with optimized token embedding and generates the customized concept image by composing the optimized token with target prompt. Dream-Booth [32] and Custom diffusion [20] has opted for fine-tuning the U-Net parameters, which results in improved subject fidelity. Another line of work has focused on exploring fast customization generation by additional encoder which requires substantial data and usually focuses on close-domain datasets such as human face. Our work mainly involves general customization and thus is compared with open-domain method Elite [45] in the experiment. In response to the limited expressiveness of spatial structures in text embeddings, several methods [4, 17, 24, 37] have explored injecting concept information at the self-attention layer. However, the generated results tend to entirely retain the reference subject, leading to the loss of text alignment. Recently, some works [3, 6] propose to distinguish identity-irrelevant attributes from identity-relevant ones. While they mainly focus on the impact of pose and background on the subject, our method prioritizes stylistic attributes.

### 3 PRELIMINARY

*Diffusion Models.* Our method is based on the pretrained Stable Diffusion (SD) [31], which is a popular text-to-image model and comprises two main components. Initially, an autoencoder with encoder  $\mathcal{E}(\cdot)$  and decoder  $\mathcal{D}(\cdot)$  learns to compress input image  $I$  into a lower-dimensional latent space  $z_0 = \mathcal{E}(I)$ , which is then decoded back into image  $\mathcal{D}(\mathcal{E}(I)) \approx I$ . Subsequently, a conditional diffusion model  $\epsilon_\theta$  is trained on this latent space to denoise noisy latent codes conditioned on textual input  $y$ . The training process involves employing a basic mean-squared loss, denoted as:

$$\mathcal{L}_{LDM} = \mathbb{E}_{z_0 \sim \mathcal{E}(I), y, \epsilon, t} [\|\epsilon - \epsilon_\theta(z_t, t, y)\|_2^2], \quad (1)$$

where  $\epsilon \sim \mathcal{N}(0, I)$  signifies unscaled noise,  $z_t$  denotes the latent state at time step  $t$ . During inference, Gaussian noise  $z_T$  is progressively diminished to  $z_0$  and then decoded back into image output.

Conditional diffusion model  $\epsilon_\theta$  of SD is based on a U-Net architecture, which comprises convolution layers, cross attention layers and self attention layers [40]. Among them, the self attention layers capture the spatial relationship of image features within themselves. Formally, after projecting the latent features in timestep  $t$  into queries  $q_t$ , keys  $k_t$  and values  $v_t$ , the self attention calculation is expressed as follows:

$$\text{SA}(q_t, k_t, v_t) = \text{SoftMax}\left(\frac{q_t k_t^T}{\sqrt{d}}\right)v_t, \quad (2)$$

where  $d$  is the feature dimension of  $q_t$ ,  $k_t$ , and  $v_t$ .

*Image Customization.* Image customization [1, 11, 12, 20, 24, 32, 43] learns a trainable text embedding  $S^*$  to represent the specific concept based on user-provided concept images. Leveraging  $S^*$ , novel images embodying the desired concept can be synthesized under diverse textual descriptions. Previous methods [20, 24, 32] further enhance concept representation during optimization by

updating weights of projection matrix of key and value in the cross-attention layer or the entire U-Net’s parameters. To effectively integrate  $S^*$  into the generative process, the input text prompt  $y$  is formulated as ‘Photo of a  $S^*$  [class]’, where [class] corresponds to the specific class name of the designated concept.

*Image Fourier Transformation.* The Fourier transform of images constitutes a fundamental technique widely used in image processing and computer vision fields [19, 22, 27, 35]. It serves as a powerful tool for analyzing the frequency components of an image and extracting important features for various applications. For an image  $I \in \mathbb{R}^{H \times W \times C}$ , the Fourier transform is defined as:

$$\mathcal{F}(I)(u, v) = \frac{1}{\sqrt{HW}} \sum_{h=0}^{H-1} \sum_{w=0}^{W-1} I(h, w) e^{-j2\pi\left(\frac{h}{H}u + \frac{w}{W}v\right)}, \quad (3)$$

where  $\mathcal{F}$  denotes the frequency-domain representation of the image and  $\mathcal{F}^{-1}$  signifies the corresponding inverse Fourier transformation. High-pass and low-pass filters are conventionally applied to the frequency-domain representation of images to isolate specific frequency bands. The high-pass filter, denoted as  $H(u, v)$ , serves to suppress low-frequency components while retaining high-frequency details. Conversely, the low-pass filter  $L(u, v)$  is designed to preserve low-frequency information while mitigating high-frequency noise. These filters are formulated as follows:

$$H(u, v) = \begin{cases} 0 & \text{if } \sqrt{(u - u_0)^2 + (v - v_0)^2} \leq f_c \\ 1 & \text{if } \sqrt{(u - u_0)^2 + (v - v_0)^2} > f_c \end{cases}, \quad (4)$$

$$L(u, v) = 1 - H(u, v),$$

where  $(u_0, v_0)$  represents the center of the Fourier frequency map and  $f_c$  is the cutoff frequency. In our work, we utilize Fourier transformation to acquire conceptual images characterized by high and low frequencies, subsequently leveraging them to enhance the model’s denoising capacity across various frequency spectra.

## 4 METHODOLOGY

### 4.1 Frequency-aware Decoupled Textual Embedding

Essentially, conventional methods for customizing images through fine-tuning rely on a single text embedding and diffusion learning process applied to the original image to capture image concept. However, these approaches struggle to adapt the concept representation derived from text embedding to customize images under significantly different stylized textual descriptions from the original image. We attribute this challenge to the model’s failure to explicitly decouple image content from semantic style during the concept learning process, resulting in a tightly coupled representation. Consequently, we propose Frequency-aware Decoupled Textual Embedding to address this issue. FDTE decouples high-frequency style and low-frequency content information from a frequency-domain perspective, thereby learning and reinforcing separate conceptual representations of content and style through corresponding diffusion learning processes on different frequency bands. As shown in fig. 2, FDTE first transforms the original image  $I_{ori}^g$  into high-frequency and low-frequency components  $I_{HF}^g$  and  $I_{LF}^g$  through image Fourier transformation, accompanied by two

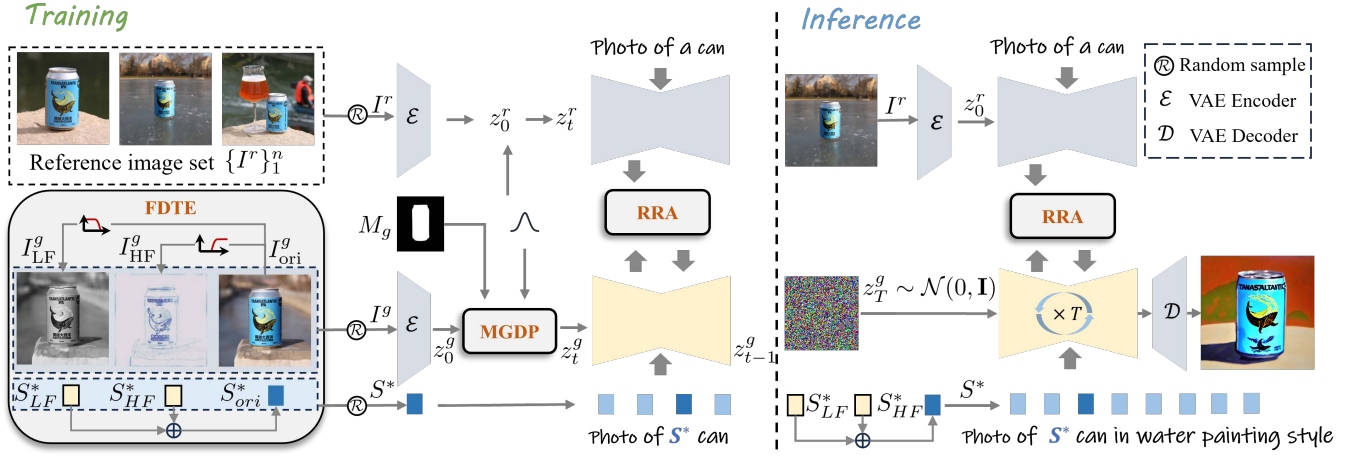


**Figure 2: Method overview.** In the training stage, the Frequency-aware Decoupled TextualEmbedding (FDTE) decomposes the original image  $I_{ori}^g$  into low frequency (LF) and high frequency (HF) bands, which are selectively formed into the input of denoising UNet along with their corresponding text embeddings including  $S_{LF}^*$  and  $S_{HF}^*$ . After encoding into the latent space, the target features undergo forward diffusion added with noise in Mask Guided Diffusion Process (MGDP), thereby mitigating the impact of background elements. Subsequently, Residual Reference Attention (RRA) integrates spatial details from the reference image  $I^r$  into the result to enhance image consistency. During inference, we first generate corresponding spatial domain embedding  $S^*$  by optimized high-frequency and low-frequency text embeddings. Then, the sampled Gaussian noise  $z_T^g$  is iteratively denoised into generation result aligned with the text for  $T$  steps.

learnable text embeddings  $S_{HF}^*$  and  $S_{LF}^*$  to indicate respective denoising conditions. Specifically,  $S_{HF}^*$  encapsulates considerations regarding high-frequency aware style attribute, while  $S_{LF}^*$  attends to low-frequency content attribute. Additionally, to maintain denoising efficacy for the original image  $I_{ori}^g$ , we retain it as a candidate input for the model, represented by textual embeddings  $S_{ori}^*$  that calculated by the sum of frequency-aware embeddings. Formally, the input candidates of denoising model are denoted as follows:

$$I_g = \mathcal{R}_{p_l, p_h, p_o} [L(\mathcal{F}(I_{ori}^g)), H(\mathcal{F}(I_{ori}^g)), I_{ori}^g],$$

$$S^* = \mathcal{R}_{p_l, p_h, p_o} [S_{LF}^*, S_{HF}^*, S_{ori}^*], \text{ where } S_{ori}^* = S_{LF}^* + S_{HF}^*, \quad (5)$$

where the operation symbolized by  $\mathcal{R}_{p_l, p_h, p_o} [\cdot, \cdot, \cdot]$  entails the random selection of one of the three candidates based on probabilities  $p_l, p_h, p_o$  to serve as the output. During the training phase, these inputs are randomly selected to constitute  $I_g$ , from which the latent encoding  $z_0^g$  is derived. Subsequently, their corresponding text embeddings, which respectively represent high-frequency perception, low-frequency perception, and the original image, are integrated into the fine-tuning process. Notably, during the inference stage, the text embedding  $S_{ori}^*$  corresponding to the original image serves as a conditional input to ensure that the generated outcomes adhere closely to real images.

## 4.2 Mask Guided Diffusion Process

While FDTE aids in diminishing the model's reliance on the original image style, direct learning of conceptual representations during the image diffusion process may be interfered by subject-irrelevant

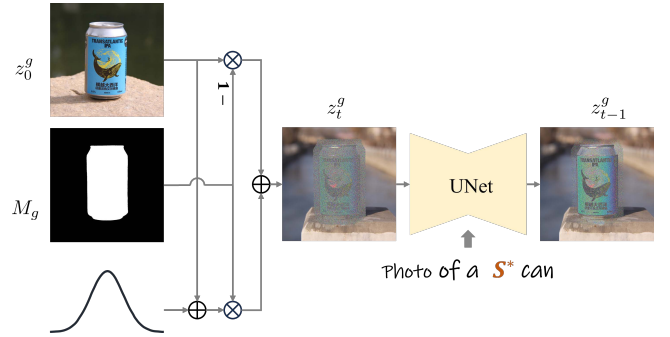


**Figure 3: Illustration of Mask Guided Diffusion Process.** To eliminate background interference on the concept representation  $S^*$ , we exclusively apply noise addition and prediction to the subject region indicated by subject mask  $M_g$ .

background attribute. Although previous works [2, 20] have explored strategies wherein the computation of diffusion loss is confined exclusively within the subject region guided by accurate mask, the generated results are not promising as shown in fig. 8. Inspired by SmartBrush [46], we propose a mask-guided diffusion process guided by the subject mask  $M_g$ , thus compelling the model to focus on learning the conceptual representation of the subject itself. Specifically, as shown in fig. 3, we conduct noise addition and prediction within the subject mask region in the diffusion process and retain clean background information inputted into UNet, which prompts the learning of subject concept. Mathematically, the input



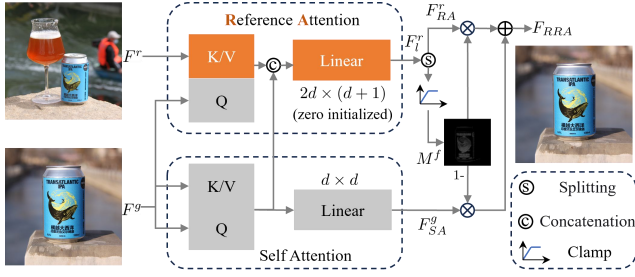


Figure 4: Framework of Residual Reference Attention (RRA).

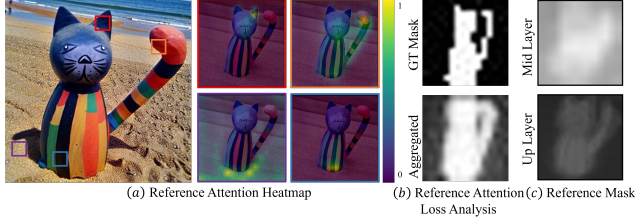


Figure 5: (a) Reference Attention is capable of attending to reasonable texture information from reference features. (b) The aggregated reference attention map closely reassembles the ground truth subject mask during  $\mathcal{L}_{ra}$  calculation eq. (10). (c) Reference Mask  $M^f$  predicted in RRA accurately distinguishes the subject from the background.

noisy latent of UNet is formulated as follows:

$$z'_t = M_g * z_t + (1 - M_g) * z_0, \quad (6)$$

Finally, we reformulate the denoising objective to be aligned with masked diffusion loss [2] and express it as follows:

$$\mathcal{L}_{Mask-LDM} = \mathbb{E}_{z_0 \sim \mathcal{E}(I), y, \epsilon, t} \left[ M_g * \left\| \epsilon - \epsilon_\theta(z'_t, t, y) \right\|_2^2 \right]. \quad (7)$$

### 4.3 Residual Reference Attention

As illustrated in fig. 4, we propose Residual Reference Attention to enhance image alignment by incorporating spatial details of the subject from reference image with reference attention. In the training process of the model, the features of the reference image  $I^r$  are initially encoded to obtain the latent code  $z_0^r$ , which is then perturbed with Gaussian noise of  $t$  step to obtain  $z_t^r$ . This noisy latent code is then fed into a frozen SD UNet  $\epsilon_r$ . Before the self-attention module of  $\epsilon_r$ , reference features are extracted and merged with the corresponding features at the positions of UNet  $\epsilon_\theta$  containing trainable parameters through RRA, ensuring the proximity and effectiveness of feature fusion in the feature space. During the inference phase, features from the reference image are injected into the denoising network, gradually incorporating spatial information from the reference image during the denoising process over  $T$  steps.

In typical personalized tasks, occlusions and variations in view-point often occur between reference images and generated results. Consequently, simple fusion of reference image features may introduce interference. Previous approaches [17, 24] only focused on the foreground regions of the subject, neglecting the influence

of backgrounds and mismatched foregrounds, or requiring additional forward processes [4] during inference to obtain the subject's mask for fusion. To address this issue and mitigate additional inference overhead, RRA learns explicit fusion masks and adaptively determines fusion coefficients during the optimization process. As illustrated in Figure fig. 4, RRA projects reference appearance features  $F^r \in \mathbb{R}^{hw \times d}$  into keys and values, sharing the same queries from target features  $F^g \in \mathbb{R}^{hw \times d}$  within the corresponding self-attention modules. Subsequently, the attention computation results from both reference attention and self attention modules are concatenated as inputs for reference mask  $M^f$  prediction and feature calculation, which is formulated as follows

$$F_l^r = \mathcal{H}_r([\text{SA}(F^g, F^r, F^r), \text{SA}(F^g, F^g, F^g)])$$

$$F_{RA}^r * M^f = \langle F_l^r \rangle_{0:d} \cdot \phi(\langle F_l^r \rangle_{d:d+1}) \quad (8)$$

$$F_{SA}^g = \mathcal{H}_s(\text{SA}(F^g, F^g, F^g)),$$

where  $\langle \cdot \rangle$  and  $[\cdot]$  mean the feature splitting and concatenation operations, respectively.  $\phi(\cdot)$  denotes the clamp function, constraining the results to the interval (0, 1) for generating reference mask  $M^f$  as visualized in fig. 5 (c). Reference attention mask  $M^f \in \mathbb{R}^{hw \times 1}$  and reference feature  $F_{RA}^r \in \mathbb{R}^{hw \times d}$  are calculated by linear layer  $\mathcal{H}_r : \mathbb{R}^{2d} \rightarrow \mathbb{R}^{d+1}$ , which is trainable and zero initialized to promote the training stability at the beginning. The target feature  $F_{SA}^g$  is acquired by frozen linear layer  $\mathcal{H}_s : \mathbb{R}^d \rightarrow \mathbb{R}^d$ . The reference attention output can be regarded as the residual information for appearance reference, which is adaptively fused to make the best use of accessible information and is conducted as follows:

$$F_{RRA} = F_{SA}^g * (1 - M^f) + F_{RA}^r * M^f. \quad (9)$$

*Reference Attention Loss.* The preservation of subject details is built on the precise correspondence learned by reference attention. To facilitate the target feature attend more relevant area in reference feature map, we introduce the Reference Attention Loss that encourages the target features within the subject area to have a high attention score distributed in the corresponding subject area of paired reference. The detailed formulation of the loss function is denoted as follows:

$$\mathcal{L}_{ra} = \left\| \sum_{j=1}^{hw} \mathcal{A}_{ij} \odot M^r - M^g \right\|_2$$

$$= \left\| \sum_{j=1}^{hw} \left\{ \text{SoftMax} \left( \frac{F^g \cdot F^{rT}}{\sqrt{d}} \right) \right\}_{ij} \odot M^r - M^g \right\|_2, \quad (10)$$

where reference attention map  $\mathcal{A} \in \mathbb{R}^{hw \times hw}$  is calculated by the target feature  $F^g$  and reference feature  $F^r$ .  $M^r \in \mathbb{R}^{hw \times 1}$  and  $M^g$  denote the subject foreground mask of reference and target image extracted by Grounded-SAM [30], respectively.  $\odot$  represents the Hadamard product. As depicted in Figure fig. 5 (b), the upper sub-figure illustrates  $M^g$ , whereas the lower sub-figure showcases the aggregated reference attention scores during the training process, denoted as the first term of  $\mathcal{L}_{ra}$ . Notably, the visual result of them closely aligns, thereby underscoring the effectiveness of reference attention loss. This affirms its capability to facilitate reference attention in better leveraging the subject information present in the reference image, consequently fostering identity preservation.

## 5 EXPERIMENTS

### 5.1 Experimental Settings

*Datasets.* Our experiment is conducted at DreamBooth dataset [32], which comprises 30 subjects spanning various categories, including both non-live and live subjects. In addition, we also include an commonly used case called "cat toy," which has been utilized in many previous works [8, 11, 24, 45]. Each subject consists of 4 to 6 images paired with 55 unstylized prompts from [24] and another 22 stylized prompts generated by LLM [26] for customization. A complete prompt list is provided in supplementary material.

*Metrics.* Our evaluation follows the same setup and calculation procedures as CustomDiffusion [20], which employs three common metrics to assess the effectiveness of models in aligning text and images: CLIP-T, CLIP-I, and DINO-I. CLIP-T measures text-alignment by the feature similarity between the CLIP [28] visual representation of the generated image and the CLIP textual representation of the corresponding prompt. For the image-alignment assessment, CLIP-I and DINO-I are used to evaluate the visual similarity between generated image and concept image using the features extracted from pretrained CLIP and DINO [5] models.

*Implementation Details.* We follow previous method [32] to employ Stable Diffusion v1.4 as the text-to-image model for fair comparison. Our model is trained by an A100 GPU with the AdamW optimizer [21] for 600 steps and the learning rate is set to  $1e-5$ . Data augmentation techniques are applied to reference images to enhance the disparity with the denoising image, including image cropping, rotation, and flipping, etc. During the inference phase, the images are generated using 50 steps of DDIM [36] with classifier-free guidance scale set to 12.5.

### 5.2 Qualitative Evaluation

The qualitative comparison results with prior methods are presented in fig. 6. As can be seen, our method achieves superior customization performance in stylized prompt alignment and subject identity preservation. For textual stylization alignment, our approach excels in handling various challenging stylistic descriptions compared to existing methods. In cases where the style description closely resembles the original image, our method adeptly preserves the local details of the original image while undergoing stylization (e.g, the can in the 1st row of fig. 6), thereby enhancing its identity consistency throughout the stylization process. In contrast, for more unrealistic stylistic descriptions, our method adeptly maintains crucial semantic elements of the subject while enabling flexible and intricate style editing, a tradeoff that remains elusive to other methodologies. For instance, unlike other approaches, our method successfully disentangles from the influence of the original image's style (see the 3rd, 5th, and 7th rows of fig. 6), thereby avoiding the tendency to generate outcomes resembling the original colors and style, thus demonstrating adaptability to novel stylistic descriptions. Regarding the preservation of subject identity, our method leverages the proposed RRA technique, effectively retaining the crucial texture structures of the concept. More qualitative results can be found in supplementary material.

Method	CLIP-T ( $\uparrow$ )	CLIP-I ( $\uparrow$ )	DINO-I ( $\uparrow$ )
Textual Inversion (TI) [11]	0.725	0.765	0.537
	0.742	0.698	0.418
DreamBooth [32]	<u>0.777</u>	0.788	0.616
	<b>0.795</b>	0.696	0.467
CustomDiffusion (CD) [20]	0.770	<u>0.792</u>	0.634
	0.774	0.718	0.505
ELITE [45]	0.756	0.777	0.589
	0.718	<u>0.741</u>	0.548
DreamMatcher [24]	0.768	<u>0.792</u>	<u>0.637</u>
	0.766	0.703	0.503
Ours	<b>0.782</b>	<b>0.810</b>	<b>0.670</b>
	<u>0.790</u>	<b>0.755</b>	<b>0.584</b>

**Table 1: Quantitative comparison under *unstylized* and *stylized* prompts. The best and the second best results are bold-faced and underlined.**

### 5.3 Quantitative Evaluation

Following this, we conduct a comprehensive evaluation of our method from a quantitative perspective to validate its efficacy. The baseline method for our approach is the custom diffusion. As depicted in table 1, we achieved the highest CLIP-I and DINO-I scores with both stylized and unstylized textual descriptions. This indicates that our method excels in preserving texture information of the subject and maintains superiority in retaining subject identity.

Furthermore, our method demonstrates close-to-leading results in stylized scenarios compared to Dreambooth, while exhibiting optimal CLIP-T score in non-stylized prompts, showcasing its ability for text alignment. This showcases our method's capability for superior textual editability. In summary, our method's leading performance across these metrics attests to its effectiveness in preserving subject identity and aligning with textual descriptions.

### 5.4 Ablation Study

In this section, we conduct ablation study on the core components of our method to verify their contributions. Visual comparison results of various ablation models are presented in fig. 8, while numerical analyses are provided in fig. 7. The evaluation settings of each experiment remain the same as in section 5.1.

*Effect of Residual Reference Attention and  $\mathcal{L}_{ra}$ .* Compared to the baseline, the visual results in fig. 8 indicate that the variant model B better preserves the main structural details in conceptual images after incorporating RRA, such as the patterns on jars or the appearance of cats. Additionally, improvements are observed in metrics like CLIP-I and DINO-I, which indicate enhanced subject consistency, highlighting the significant efficacy of the proposed RRA. Analysis of the reference attention heatmaps further reveals that the generated results accurately attend to corresponding positions in the reference images, validating the effectiveness of the RRA.

Moreover, reference attention loss  $\mathcal{L}_{ra}$  further improves image-alignment metrics. Visual analysis of the aggregated reference attention maps demonstrates that the subject area can effectively focus on the corresponding areas in the reference, as evidenced by the comparison between the aggregated reference attention map

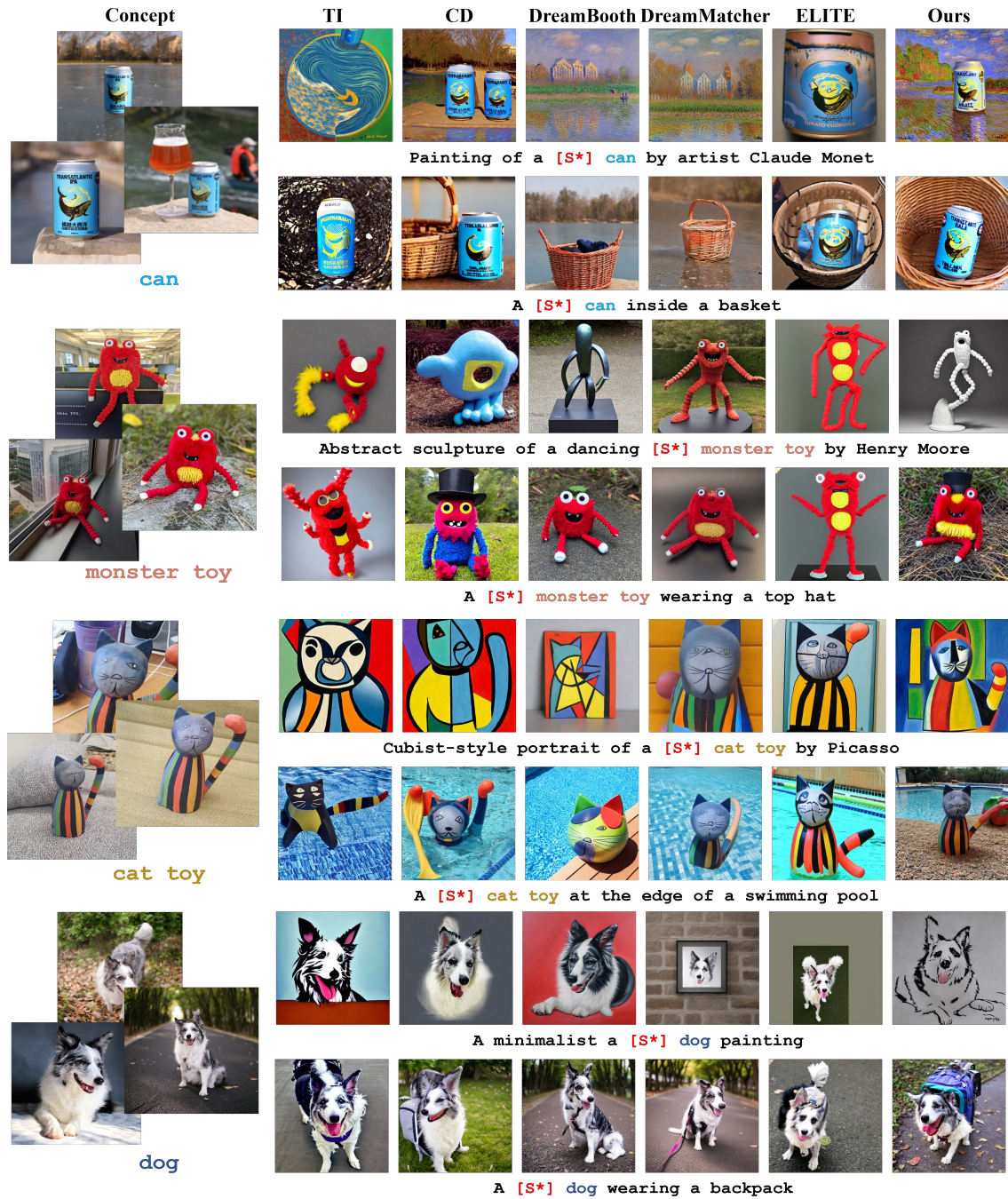


Figure 6: Qualitative comparison with prevalent methods. Please zoom in for a better view.

and the ground truth attention map in fig. 5 (B), thus proving the effectiveness of reference attention loss.

*Effect of Frequency-aware Decoupled Textual Embedding.* Subsequently, we conduct an analysis of FDTE’s impact on the effectiveness of stylized descriptions. As depicted in fig. 8, the absence of FDTE results in generated outputs that are still entrenched in the

original conceptual style, thereby struggling to conform to new stylized textual descriptions (as evidenced by the cat in fig. 8 maintaining its original image style). Conversely, FDTE facilitates the expression of stylistic effects. Additionally, FDTE also leads to a discernible enhancement in the CLIP-T score, as shown in fig. 7. This affirms FDTE’s capability in bolstering textual coherence.



	Ablation Models	CLIP-T ( $\uparrow$ )	CLIP-I ( $\uparrow$ )	DINO-I ( $\uparrow$ )
A	Baseline (CD [20])	0.770	0.792	0.634
		0.774	0.718	0.505
B	A + RRA	0.755	<u>0.822</u>	0.690
		0.746	<u>0.755</u>	<u>0.591</u>
C	B + $\mathcal{L}_{ra}$	0.755	<b>0.823</b>	<b>0.691</b>
		0.749	<b>0.757</b>	<b>0.595</b>
D	C + FDTE	0.758	0.805	0.656
		0.772	0.717	0.513
E	D + MDL [2]	0.760	0.811	0.670
		0.765	0.726	0.537
F	D + MGDP (Ours)	<b>0.782</b>	0.810	0.670
		<b>0.790</b>	<u>0.755</u>	0.584

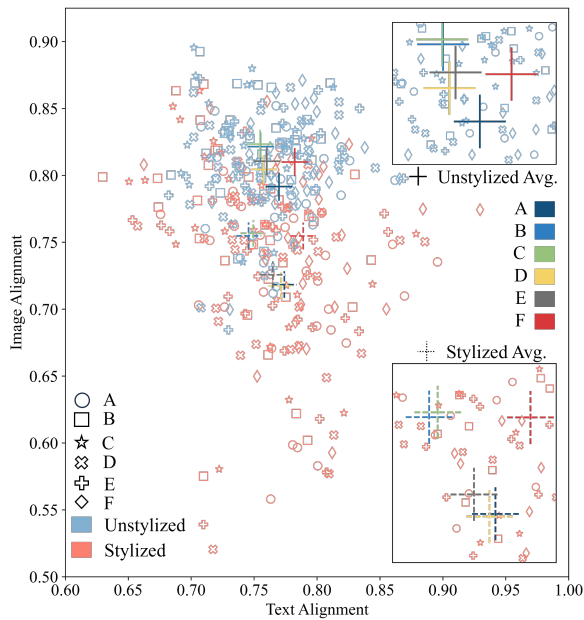


**Figure 7: The best and the second best results are bold-faced and underlined. (Upper) Numerical analysis with *unstylized* and *stylized* prompts. (Lower) Metrics across all classes are visualized, while the averaged metrics are high-lighted on the right. Compared to other model variants, our model tends towards the upper-right quadrant, indicative of achieving superior text- and image-alignment trade-offs.**

To investigate FDTE’s hyperparameter settings in detail, we analyze the probabilities of selecting high-frequency, low-frequency, and original images. For unstylized and stylized scenarios, using  $p_l, p_h, p_o = [0.1, 0.1, 0.8]$  achieves superior metrics, indicating an optimal balance between image fidelity and textual coherence.

*Effect of Mask Guided Diffusion Process.* Finally, we analyze the efficacy of MGDP in mitigating the interference of background on the generated results. As illustrated in fig. 8, RRA tends to capture spatial information from concept images directly, thereby rendering the background more similar to the conceptual image (see A and B in fig. 8). Exclusion of MGDP leads to overfitting to the concept



**Figure 8: Visualization results of ablation study.**

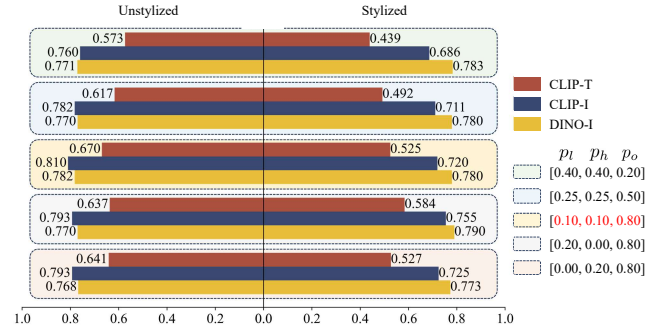


**Figure 9: Numerical analysis of FDTE.  $p_l, p_h,$  and  $p_o$  represent the probability of choosing low-frequency, high-frequency and original images, respectively.**

image’s background in the result. Although MDL introduces constraints on background regions in loss objectives, it still struggles to mitigate the influence of background attributes. Conversely, MGDP exhibits superior capability in decoupling backgrounds from the subject, aligning the generated results more closely with textual descriptions (see the galaxy background in the last column of fig. 8).

Notably, our goal is to strike a balance between aligning images and text. Although our full setting shown in the upper table of fig. 7 does not yield optimal scores across all metrics compared to other model variations, the lower figure of fig. 7 reveals that our approach is positioned closer to the upper-right quadrant. This observation demonstrates the superiority of our method in achieving the desired trade-off between image- and text-alignment.

## 6 CONCLUSION

In conclusion, we propose Equilibrated Diffusion to customize images for better image consistency and stylized text alignment. Specifically, by decoupling content and style through frequency-aware decoupled textual embedding, we decompose the original diffusion optimization process across different frequency bands. This enhances the model’s ability to understand content represented by low frequencies and style represented by high frequencies, which is guided by decoupled text embeddings and enhances text consistency expression. The mask guided diffusion process mitigates the influence of the concept image background on the results and further enhances text alignment. Moreover, the residual reference attention and reference attention loss better transfer spatial details from reference concepts, promoting texture consistency.



## REFERENCES

- [1] Yuval Alaluf, Elad Richardson, Gal Metzger, and Daniel Cohen-Or. 2023. A Neural Space-Time Representation for Text-to-Image Personalization. *ACM Transactions on Graphics (TOG)* 42, 6 (2023), 1–10.
- [2] Omri Avrahami, Kfir Aberman, Ohad Fried, Daniel Cohen-Or, and Dani Lischinski. 2023. Break-a-scene: Extracting multiple concepts from a single image. In *SIGGRAPH Asia 2023 Conference Papers*. 1–12.
- [3] Yufei Cai, Yuxiang Wei, Zhilong Ji, Jinfeng Bai, Hu Han, and Wangmeng Zuo. 2024. Decoupled textual embeddings for customized image generation. In *Proceedings of the AAAI Conference on Artificial Intelligence*, Vol. 38. 909–917.
- [4] Mingdeng Cao, Xintao Wang, Zhongang Qi, Ying Shan, Xiaohu Qie, and Yinqiang Zheng. 2023. Masactrl: Tuning-free mutual self-attention control for consistent image synthesis and editing. In *Proceedings of the IEEE/CVF International Conference on Computer Vision*. 22560–22570.
- [5] Mathilde Caron, Hugo Touvron, Ishan Misra, Hervé Jégou, Julien Mairal, Piotr Bojanowski, and Armand Joulin. 2021. Emerging properties in self-supervised vision transformers. In *Proceedings of the IEEE/CVF international conference on computer vision*. 9650–9660.
- [6] Hong Chen, Yipeng Zhang, Simin Wu, Xin Wang, Xuguang Duan, Yuwei Zhou, and Wenwu Zhu. 2023. Disenbooth: Identity-preserving disentangled tuning for subject-driven text-to-image generation. In *The Twelfth International Conference on Learning Representations*.
- [7] Wenhu Chen, Hexiang Hu, Yandong Li, Nataniel Ruiz, Xuhui Jia, Ming-Wei Chang, and William W Cohen. 2024. Subject-driven text-to-image generation via apprenticeship learning. *Advances in Neural Information Processing Systems* 36 (2024).
- [8] Jooyoung Choi, Yunyei Choi, Yunji Kim, Junho Kim, and Sungroh Yoon. 2023. Custom-edit: Text-guided image editing with customized diffusion models. *arXiv preprint arXiv:2305.15779* (2023).
- [9] Siying Cui, Jiankang Deng, Jia Guo, Xiang An, Yongle Zhao, Xinyu Wei, and Ziyong Feng. 2024. IDAdapter: Learning Mixed Features for Tuning-Free Personalization of Text-to-Image Models. *arXiv preprint arXiv:2403.13535* (2024).
- [10] Ziyi Dong, Pengxu Wei, and Liang Lin. 2022. DreamArtist: Towards Controllable One-Shot Text-to-Image Generation via Positive-Negative Prompt-Tuning. *arXiv preprint arXiv:2211.11337* (2022).
- [11] Rinon Gal, Yuval Alaluf, Yuval Atzmon, Or Patashnik, Amit Haim Bermano, Gal Chechik, and Daniel Cohen-Or. 2023. An Image is Worth One Word: Personalizing Text-to-Image Generation using Textual Inversion. In *The Eleventh International Conference on Learning Representations*. <https://openreview.net/forum?id=NAQvF08TcyG>
- [12] Rinon Gal, Moab Arar, Yuval Atzmon, Amit H Bermano, Gal Chechik, and Daniel Cohen-Or. 2023. Encoder-based domain tuning for fast personalization of text-to-image models. *ACM Transactions on Graphics (TOG)* 42, 4 (2023), 1–13.
- [13] Ligong Han, Yinxiao Li, Han Zhang, Peyman Milanfar, Dimitris Metaxas, and Feng Yang. 2023. Svdif: Compact parameter space for diffusion fine-tuning. In *Proceedings of the IEEE/CVF International Conference on Computer Vision*. 7323–7334.
- [14] Shaozhe Hao, Kai Han, Shihao Zhao, and Kwan-Yee K Wong. 2023. ViCo: Plug-and-play Visual Condition for Personalized Text-to-image Generation. (2023).
- [15] Feihong He, Gang Li, Mengyuan Zhang, Leilei Yan, Lingyu Si, and Fanzhang Li. 2024. Freestyle: Free lunch for text-guided style transfer using diffusion models. *arXiv preprint arXiv:2401.15636* (2024).
- [16] Jonathan Ho, Ajay Jain, and Pieter Abbeel. 2020. Denoising diffusion probabilistic models. *Advances in neural information processing systems* 33 (2020), 6840–6851.
- [17] Miao Hua, Jiawei Liu, Fei Ding, Wei Liu, Jie Wu, and Qian He. 2023. Dream-Tuner: Single Image is Enough for Subject-Driven Generation. *arXiv preprint arXiv:2312.13691* (2023).
- [18] Xuhui Jia, Yang Zhao, Kelvin CK Chan, Yandong Li, Han Zhang, Boqing Gong, Tingbo Hou, Huisheng Wang, and Yu-Chuan Su. 2023. Taming encoder for zero fine-tuning image customization with text-to-image diffusion models. *arXiv preprint arXiv:2304.02642* (2023).
- [19] Liming Jiang, Bo Dai, Wayne Wu, and Chen Change Loy. 2021. Focal frequency loss for image reconstruction and synthesis. In *Proceedings of the IEEE/CVF international conference on computer vision*. 13919–13929.
- [20] Nupur Kumari, Bingliang Zhang, Richard Zhang, Eli Shechtman, and Jun-Yan Zhu. 2023. Multi-concept customization of text-to-image diffusion. In *Proceedings of the IEEE/CVF Conference on Computer Vision and Pattern Recognition*. 1931–1941.
- [21] Ilya Loshchilov and Frank Hutter. 2017. Decoupled weight decay regularization. *arXiv preprint arXiv:1711.05101* (2017).
- [22] Liyuan Ma, Tingwei Gao, Haibin Shen, and Kejie Huang. 2023. Freqhpt: Frequency-aware attention and flow fusion for human pose transfer. In *Proceedings of the IEEE/CVF Conference on Computer Vision and Pattern Recognition*. 3490–3495.
- [23] Yiyang Ma, Huan Yang, Wenjing Wang, Jianlong Fu, and Jiaying Liu. 2023. Unified multi-modal latent diffusion for joint subject and text conditional image generation. *arXiv preprint arXiv:2303.09319* (2023).
- [24] Jisu Nam, Heesu Kim, Dongjae Lee, Siyoon Jin, Seungryong Kim, and Seunggyu Chang. 2024. DreamMatcher: Appearance Matching Self-Attention for Semantically-Consistent Text-to-Image Personalization. *arXiv preprint arXiv:2402.09812* (2024).
- [25] Alex Nichol, Prafulla Dhariwal, Aditya Ramesh, Pranav Shyam, Pamela Mishkin, Bob McGrew, Ilya Sutskever, and Mark Chen. 2021. Glide: Towards photorealistic image generation and editing with text-guided diffusion models. *arXiv preprint arXiv:2112.10741* (2021).
- [26] R OpenAI. 2023. Gpt-4 technical report. arxiv 2303.08774. *View in Article* 2, 5 (2023).
- [27] Zhongwei Qiu, Huan Yang, Jianlong Fu, and Dongmei Fu. 2022. Learning spatiotemporal frequency-transformer for compressed video super-resolution. In *European Conference on Computer Vision*. Springer, 257–273.
- [28] Alec Radford, Jong Wook Kim, Chris Hallacy, Aditya Ramesh, Gabriel Goh, Sandhini Agarwal, Girish Sastry, Amanda Askell, Pamela Mishkin, Jack Clark, et al. 2021. Learning transferable visual models from natural language supervision. In *International conference on machine learning*. PMLR, 8748–8763.
- [29] Aditya Ramesh, Prafulla Dhariwal, Alex Nichol, Casey Chu, and Mark Chen. 2022. Hierarchical text-conditional image generation with clip latents. *arXiv preprint arXiv:2204.06125* 1, 2 (2022), 3.
- [30] Tianhe Ren, Shilong Liu, Ailing Zeng, Jing Lin, Kunchang Li, He Cao, Jiayu Chen, Xinyu Huang, Yukang Chen, Feng Yan, et al. 2024. Grounded sam: Assembling open-world models for diverse visual tasks. *arXiv preprint arXiv:2401.14159* (2024).
- [31] Robin Rombach, Andreas Blattmann, Dominik Lorenz, Patrick Esser, and Björn Ommer. 2022. High-resolution image synthesis with latent diffusion models. In *Proceedings of the IEEE/CVF Conference on Computer Vision and Pattern Recognition*. 10684–10695.
- [32] Nataniel Ruiz, Yuanzhen Li, Varun Jampani, Yael Pritch, Michael Rubinstein, and Kfir Aberman. 2023. Dreambooth: Fine tuning text-to-image diffusion models for subject-driven generation. In *Proceedings of the IEEE/CVF Conference on Computer Vision and Pattern Recognition*. 22500–22510.
- [33] Chitwan Saharia, William Chan, Saurabh Saxena, Lala Li, Jay Whang, Emily L Denton, Kamyar Ghasemipour, Raphael Gontijo Lopes, Burcu Karagol Ayan, Tim Salimans, et al. 2022. Photorealistic text-to-image diffusion models with deep language understanding. *Advances in neural information processing systems* 35 (2022), 36479–36494.
- [34] Jing Shi, Wei Xiong, Zhe Lin, and Hyun Joon Jung. 2023. Instantbooth: Personalized text-to-image generation without test-time finetuning. *arXiv preprint arXiv:2304.03411* (2023).
- [35] Chenyang Si, Weihao Yu, Pan Zhou, Yichen Zhou, Xinchao Wang, and Shuicheng Yan. 2022. Inception transformer. *Advances in Neural Information Processing Systems* 35 (2022), 23495–23509.
- [36] Jiaming Song, Chenlin Meng, and Stefano Ermon. 2020. Denoising diffusion implicit models. *arXiv preprint arXiv:2010.02502* (2020).
- [37] Yeji Song, Jimyeong Kim, Wonhark Park, Wonsik Shin, Wonjong Rhee, and Nojun Kwak. 2024. Harmonizing Visual and Textual Embeddings for Zero-Shot Text-to-Image Customization. *arXiv preprint arXiv:2403.14155* (2024).
- [38] Yang Song, Jascha Sohl-Dickstein, Diederik P Kingma, Abhishek Kumar, Stefano Ermon, and Ben Poole. 2020. Score-based generative modeling through stochastic differential equations. *arXiv preprint arXiv:2011.13456* (2020).
- [39] Yoad Twel, Rinon Gal, Gal Chechik, and Yuval Atzmon. 2023. Key-locked rank one editing for text-to-image personalization. In *ACM SIGGRAPH 2023 Conference Proceedings*. 1–11.
- [40] Ashish Vaswani, Noam Shazeer, Niki Parmar, Jakob Uszkoreit, Llion Jones, Aidan N Gomez, Łukasz Kaiser, and Illia Polosukhin. 2017. Attention is all you need. *Advances in neural information processing systems* 30 (2017).
- [41] Andrey Voynov, Kfir Aberman, and Daniel Cohen-Or. 2023. Sketch-guided text-to-image diffusion models. In *ACM SIGGRAPH 2023 Conference Proceedings*. 1–11.
- [42] Andrey Voynov, Qinghao Chu, Daniel Cohen-Or, and Kfir Aberman. 2023. P+: Extended Textual Conditioning in Text-to-Image Generation. *arXiv preprint arXiv:2303.09522* (2023).
- [43] Qixun Wang, Xu Bai, Haofan Wang, Zekui Qin, and Anthony Chen. 2024. Instantid: Zero-shot identity-preserving generation in seconds. *arXiv preprint arXiv:2401.07519* (2024).
- [44] Weilun Wang, Jianmin Bao, Wengang Zhou, Dongdong Chen, Dong Chen, Lu Yuan, and Houqiang Li. 2022. Semantic image synthesis via diffusion models. *arXiv preprint arXiv:2207.00050* (2022).
- [45] Yuxiang Wei, Yabo Zhang, Zhilong Ji, Jinfeng Bai, Lei Zhang, and Wangmeng Zuo. 2023. Elite: Encoding visual concepts into textual embeddings for customized text-to-image generation. In *Proceedings of the IEEE/CVF International Conference on Computer Vision*. 15943–15953.
- [46] Shaoran Xie, Zhifei Zhang, Zhe Lin, Tobias Hinz, and Kun Zhang. 2023. Smartbrush: Text and shape guided object inpainting with diffusion model. In *Proceedings of the IEEE/CVF Conference on Computer Vision and Pattern Recognition*. 22428–22437.
- [47] Hu Ye, Jun Zhang, Sibio Liu, Xiao Han, and Wei Yang. 2023. Ip-adapter: Text compatible image prompt adapter for text-to-image diffusion models. *arXiv preprint arXiv:2308.06721* (2023).